

Nafamostat reduces systemic inflammation in TLR7-mediated virus-like illness

Abi G. Yates (✉ abi.yates@oriel.ox.ac.uk)

University of Oxford <https://orcid.org/0000-0002-8501-2160>

Caroline M. Weglinski

University of Oxford Medical Sciences Division

Yuxin Ying

University of Oxford Medical Sciences Division

Tatyana Strekalova

University of Maastricht: Universiteit Maastricht

Daniel C. Anthony

University of Oxford Medical Sciences Division <https://orcid.org/0000-0003-1380-6655>

Research Article

Keywords: Nafamostat, viral infection, inflammation, sickness behaviour, COVID-19

Posted Date: June 16th, 2021

DOI: <https://doi.org/10.21203/rs.3.rs-628384/v1>

License:   This work is licensed under a Creative Commons Attribution 4.0 International License.

[Read Full License](#)

Version of Record: A version of this preprint was published at Journal of Neuroinflammation on January 6th, 2022. See the published version at <https://doi.org/10.1186/s12974-021-02357-y>.

Abstract

Background: The serine protease inhibitor nafamostat has been proposed as a treatment for COVID-19, by inhibiting TMPRSS2-mediated viral cell entry. Nafamostat has been shown to have other, immunomodulatory effects, which may be beneficial for treatment, however animal models of ssRNA virus infection are lacking. In this study, we examined the potential of the dual TLR7/8 agonist R848 to mimic the host response to a ssRNA virus infection and the associated behavioural response. In addition, we evaluated the anti-inflammatory effects of nafamostat in this model.

Methods: CD-1 mice received an intraperitoneal injection of R848 (200µg, prepared in DMSO, diluted 1:10 in saline) or diluted DMSO alone, and an intravenous injection of either nafamostat (100µL, 3mg/kg in saline) or saline. Sickness behaviour was determined by temperature, food intake, sucrose preference test, open field and forced swim test. Blood and fresh liver, lung and brain were collected 6 hours post-challenge to measure markers of peripheral and central inflammation by blood analysis and qPCR.

Results: R848 induced a robust inflammatory response, as evidenced by increased expression of TNF, IFN-γ, CXCL1 and CXCL10 in the liver, lung and brain, as well as a sickness behaviour phenotype. Exogenous administration of nafamostat suppressed the hepatic inflammatory response, significantly reducing TNF and IFN-γ expression, but had no effect on lung or brain cytokine production. R848 administration depleted circulating leukocytes, which was restored by nafamostat treatment.

Conclusions: Our data indicate that R848 administration provides a useful model of ssRNA virus infection, which induces inflammation in the periphery and CNS, and virus infection-like illness. In turn, we show that nafamostat has a systemic anti-inflammatory effect, in the presence of the TLR7/8 agonist. Therefore, the results indicate that nafamostat has anti-inflammatory actions, beyond its ability to inhibit TMPRSS2, that might potentiate its anti-viral actions in pathologies such as COVID-19.

Introduction

The serine protease inhibitor nafamostat is in clinical trials as a potential treatment for COVID-19, owing to its ability to inhibit TMPRSS2-mediated viral entry of SARS-CoV2 into lung epithelial cells [1, 2]. Indeed, nafamostat was identified as a potential therapy using a Dual Split Protein reporter fusion assay to screen a library consisting of 1,017 FDA-approved drugs able to prevent MERS-CoV S protein-initiated membrane fusion, a similar coronavirus, from infecting cells in this way [3]. This screening result, together with experimental data from MERS-CoV infection of cultured airway epithelial cell-derived Calu-3 cells, highlighted that nafamostat, over all other screened compounds, could be effective at inhibiting viral entry. Further evidence for the use of nafamostat is because it is an inactivator of coagulation fibrinolysis, and platelet aggregation with potent inhibitory activity against thrombin, coagulation factors in active form (XIIa, Xa), kallikrein, plasmin, and complement factors (Clr, Cls). For this reason, nafamostat is used to treat disseminated intravascular coagulation (DIC) routinely in Japan [4]. However, it has also been shown to improve outcomes in models of stroke [5] and of spinal cord injury [6], and it is also used

to treat pancreatitis [7], suggesting it has additional, immunomodulatory effects which are beneficial to the host. However, to date, its impact of virally induced inflammation is unclear.

Current models of systemic inflammation often employ bacteria-derived polysaccharides such as LPS from *E. coli* or *S. enterica*. These activate the pattern recognition receptor (PRR) toll-like receptor (TLR), which, via Myeloid differentiation primary response (MyD) 88, causes NF- κ B translocation to the nucleus and upregulation of central and peripheral cytokines expression [8]. The host response to TLR agonists has evolved to recognise and protect the individual from the full spectrum of infectious agents. A common feature of TLR activation is the acute phase response (APR) and the generation of liver derived acute phase proteins (APP), which mobilise leukocytes, such as neutrophils from the spleen and bone marrow to the circulation and then to the site of infection to eliminate the pathogen [9]. The expression profile of the APPs is dependent on the nature of the pathogen and the TLR signalling pathways that activated. Typically, the APR is associated with the production of pentraxins, such as CRP, serum amyloid-A, and the expression of cytokines such as IL-1 β , TNF and IL-6, and chemokines such as CXCL1, CCL2 and CXCL10 (PMID: 15855648). However, the production of peripheral cytokines is also associated with *de novo* cytokine expression in the brain. As a consequence, behavioural responses, termed sickness behaviours, are induced owing to the expression of central cytokines [10]. These behaviours are characterised by reduced activity, anorexia, and decreased motivational and goal directed activity [11]. These inflammatory and behavioural responses are evident following both bacterial and viral infection [12], however the responses are coordinated via different signalling pathways [13].

RNA viruses are detected by PRRs recognising either single-stranded, such as SARS-CoV-2, or double-stranded RNA, such as reoviruses [14]. Single-stranded or double-stranded RNA are detected by TLR7/8 or TLR3, respectively, and trigger distinct downstream responses. The TLR3 pathway is MyD88-independent and induces a type-1 interferon response, driven largely by the transcription factor IRF3 and designed to induce the proliferation of antigen-specific CD8 + T-cells. The inflammatory response to TLR7/8 stimulation also induces type-1 interferon, but it is initiated by the transcription factor IRF7, which is expressed at much lower levels than the more ubiquitous IRF3 [15]. Activation of TLR7 triggers a MyD88-dependent cascade, involving interleukin-1 receptor-associated kinase 1 (IRAK-1), IRAK-4, and TNF receptor-associated factor 6 (TRAF6), which leads to NF κ B and IRF7 activation [14]. Phosphorylated IRF-7 then upregulates the production of the type I interferons (IFNs), such as IFN α and IFN β . Although stimulation of both TLR3 and TLR7/8 induces inflammation, the differences in the underlying mechanisms are large enough to justify exploration of the consequence of a TLR7/8 mediated event, independent of TLR3 signalling *in vivo*.

In vivo models of viral infection use molecules specifically designed to target PRRs. This approach is safer than using live or attenuated viruses, avoiding the associated health risks, and allows greater control of the inflammatory response with dosage manipulation. The most common model uses polyinosinic:polycytidylic acid (polyI:C), a synthetic double-stranded RNA, which thus stimulates TLR3 [12]. However, this fails to replicate the stimulation which occurs from single-stranded RNA viruses such as SARS-CoV2, and, therefore, a more appropriate TLR7/8-mediated inflammatory model is needed. R848

(resiquimod), is known to stimulate TLR7/8, resulting in increased pro-inflammatory gene expression *in vitro*, and acute weight loss, reduced food intake and reduced locomotor activity *in vivo* [16]. However, the effects of R848, in terms of both the systemic and central inflammatory responses, and the behavioural effects of TLR7/8 stimulation require further characterisation.

The principal aims of this paper were to investigate the effects of R848 on acute behaviour and the systemic and central inflammatory responses, as well as to evaluate the potential for nafamostat to counteract the actions of TLR7/8 activation.

Methods

Animals

Male CD-1 mice, 9 weeks of age (39-40g) were purchased from Charles River (Oxford, UK) and allowed to acclimatise for 5 days before experimentation. Animals were housed in a pathogen-free facility, under standard diurnal lighting conditions (lights on 6am-6pm) with *ad libitum* access to food and water. Two cohorts were used for this study; one cohort was used for behavioural analysis and the other was used for leukocyte and qPCR analysis. Animals for behavioural analysis were given water with 1% sucrose during acclimatisation to train for sucrose preference test (SPT). Animals were housed n = 4 per cage, but separated and individually housed on the day of the experiment. All experiments were approved by the University of Oxford local committees (LERP, ACER) in accordance with the UK Animals (Scientific Procedures) Act 1989 and were performed in compliance with the ARRIVE guidelines.

Challenge

Stock R848 (resiquimod, Enzo Life Sciences, UK) was prepared by diluting in dimethyl sulfoxide (DMSO) (Sigma-Aldrich, UK) to a concentration of 10mg/mL. Stock R848 was then diluted 1:10 in sterile saline to 1mg/mL and 200µL of the working solution was injected intraperitoneally (200µg of R848 per mouse). Control animals received a 200µL intraperitoneal injection of the vehicle DMSO diluted 1:10 in sterile saline. Naïve animals that received no injections were used to establish baseline. All animals were culled 6 hours post-challenge.

Nafamostat treatment

100µL of Nafamostat (3mg/kg) (Sigma-Aldrich, UK) in 5% dextrose was injected intravenously at the time of challenge. Control animals received an intravenous injection of 5% dextrose alone.

Behaviour

To determine the effect of R848 and nafamostat on sickness behaviour, food intake during the 6-hour experiment was recorded. Immediately after the challenge, mice were given a mass of food which was weighed before (t0) and after (at 6 hours) the experiment. The difference in weight, indicating that consumed by the animals, was calculated. In addition, SPT, open field (OF) and forced swim test (FST) were performed. For SPT, animals were given access to 2 bottles, one containing normal water and one containing 1% sucrose, for the 6-hour duration of the experiment. To prevent location bias, bottles were

switched 3 hours post-challenge [11]. Total sucrose water intake (mL) and sucrose preference ($\text{volume}[\text{sucrose water}]/\text{volume}[\text{sucrose} + \text{normal water}] \times 100$) were determined. OF analysis was performed 4 hours post-challenge. Animals were placed in the corner of the apparatus and allowed to explore for 5 minutes. The number of grid crossings and rears, and time spent in the centre was recorded. FST was performed immediately prior to culling as a single FST session has been shown not to change stress markers when mice are killed 10 min thereafter (PMID: 27478647). Animals were placed into water (maintained at 29–31°C to avoid bias caused by invigorating effects of cold water) and allowed to swim for 5 minutes. For analysis, the first 2 minutes of swimming was disregarded; the latency to float and total float time were measured. OF and FST analysis were completed in a blinded fashion. Summary of behaviour tests completed is visualised in Fig. 1.

Temperature and tissue collection

Mice were anaesthetised with isoflurane and surface temperature was determined with FLIR B360 thermal imaging camera (FLIR Systems, UK). Blood was then collected by cardiac puncture, transferred into an EDTA-coated tube, and immediately analysed for leukocyte analysis. Animals were then intracardially perfused with cold, heparinised saline, and fresh liver, lung and brain were collected and snap-frozen.

Blood analysis

Approximately 200µL of blood was collected for leukocyte analysis. Within 20 minutes of collection, blood was measured in triplicate on the ABX Pentra 60 (Horiba, UK). Total leukocyte concentration, and % lymphocytes, monocytes, neutrophils, basophils and eosinophils were recorded. Data was analysed and presented as 10^3 cells per µL of blood ($\text{K}/\mu\text{L}$).

RNA extraction and cDNA conversion

RNA was extracted from fresh liver, lung and frontal cortex of the brain, using the Qiagen RNeasy Mini kit, according to manufacturer's instructions. RNA concentration was measured using a NanoDrop (Thermo Scientific, UK) and 1000ng of RNA was converted to cDNA with the Applied Biosystem's High Capacity cDNA conversion kit, following the manufacturer's instructions.

qPCR

Real-time qPCR was performed with samples in duplicate (25ng/well) using SYBR green qPCR master mix (PrimerDesign) with the Roche LightCycler 480. Primers for TNF (F: AGCCAGGAGGGAGAACAGA, R: CAGTGAGTGAAAGGGACAGAAC), IFN- γ (F: ACAGCAAGGCGAAAAAGGATG, R: TGGTGGACCACTCGGATGA), CXCL1 (F: GCTGGGATTCACCTCAAGAAC, R: TGTGGCTATGACTTCGGTTTG), CXCL10 (F: CATCCCGAGCCAACCTTCC, R: CACTCAGACCCAGCAGGAT), SAA-2 (F: TGGCTGGAAAGATGGAGACAA, R: AAAGCTCTCTCTTGCATCACTG) and CRP (F: GGGTGGTGTGAAGTACGAT; R: CCAAAGACTGCTTTGCATCA) were purchased from Sigma. Relative expression was determined by the $2^{-\Delta\Delta\text{CT}}$ method, normalised to GAPDH as the housekeeping gene (PrimerDesign).

Statistical analysis

All statistical analysis was completed with GraphPad Prism 7 software. Statistical outliers as determined by the software, were excluded from analysis. Two-way analysis of variance (ANOVA) was employed, with Sidak's post-hoc test as appropriate. Results were considered significant at $p < 0.05$ with 95% confidence intervals. All quantitative data are expressed as mean \pm standard error of the mean (SEM).

Results

R848 induces sickness behaviour in mice, which is not attenuated by Nafamostat

In this study, we investigated whether R848 administration would mimic the sickness behaviours associated with viral infection [17, 18]. Following the R848 challenge, animal temperature was significantly increased, indicative of a fever (Fig. 2A; two-way ANOVA, challenge $p < 0.0001$). There was no main effect of the nafamostat ($p = 0.788$) and no significant interaction ($p = 0.788$). R848 induced a decrease in food intake over the 6-hour experiment (Fig. 2B; two-way ANOVA, challenge $p < 0.0001$). Sidak's post-hoc testing confirmed significant differences between the control and the R848-treated animals (vehicle, $p < 0.001$; nafamostat, $p < 0.0001$), independent of nafamostat treatment (main effect, $p = 0.439$; interaction, $p = 0.889$).

Anhedonia, the compromised ability to experience pleasure, was determined by the SPT. There was a main effect of the R848 challenge on total sucrose intake (Fig. 2C; two-way ANOVA, challenge $p < 0.05$), but no effect of nafamostat ($p = 0.204$) and no interaction ($p = 0.382$). When intake of sucrose water was assessed as a preference of total fluid intake, there was no main effect of the challenge or the treatment, and no interaction (Fig. 2D; two-way ANOVA, interaction $p = 0.126$, challenge $p = 0.192$, treatment $p = 0.214$).

The OF paradigm was used to measure exploratory behaviour, which is known to be affected by sickness behaviour and where an increase in activity can be interpreted as a measure of pleasurable activity in rodents and a decrease is regarded as a sign of a depressive-like behaviour [18, 19]. Following R848 administration, the number of grid crossings/minute (Fig. 2E; two-way ANOVA, challenge $p < 0.001$) and the total number of rears (Fig. 2F; two-way ANOVA, challenge $p < 0.01$) were significantly decreased. These behavioural changes were not altered by nafamostat and there were no significant interactions. Animals challenged with R848 also spent less time in the centre of the apparatus (Fig. 2G; two-way ANOVA, challenge $p < 0.001$); there was no significant effect of the nafamostat ($p = 0.210$) and no significant interaction ($p = 0.516$).

In the FST, there was no main effect of R848 challenge or nafamostat treatment on the latency to float (Fig. 2H; two-way ANOVA, challenge $p = 0.476$, treatment $p = 0.067$). However, there was a significant interaction ($p < 0.05$); R848 induced a non-significant increase in latency to float in vehicle-treated animals, however in nafamostat-treated animals, R848 induced a significant decrease (Sidak's post-hoc test, $p < 0.05$). R848 had no effect on the total float time (Fig. 2I; two-way ANOVA, challenge $p = 0.979$), but nafamostat had a main treatment effect ($p < 0.01$). There was no significant interaction ($p = 0.532$).

R848 depletes circulating leukocytes, which is partially restored by nafamostat

Analysis of the peripheral leukocyte populations revealed that R848 induced leukopenia (Fig. 3A; two-way ANOVA, interaction $p = 0.114$, challenge $p < 0.01$, treatment $p = 0.115$). In vehicle treated animals, total blood leukocytes were significantly decreased with R848 challenge compared to control (Sidak's post-hoc test, $p < 0.05$). This was normalised by nafamostat in the R848 challenged animals (Sidak's post-hoc test, $p < 0.05$). Changes in specific subtypes of leukocytes were then investigated, to explore those responsible for the total leukocyte count result. R848 administration induced a significant decrease in blood lymphocytes (Fig. 3B; two-way ANOVA, interaction $p = 0.083$, challenge $p < 0.01$, treatment $p = 0.405$). In post-hoc testing, challenge with R848 induced lymphocyte depletion in vehicle-treated animals ($p < 0.01$). There was no corresponding depletion in the nafamostat-treated animals ($p = 0.339$), although there was also no difference between the R848 groups ($p = 0.102$). Monocytes were significantly decreased in R848 animals, which was not ameliorated by nafamostat (Fig. 3C; two-way ANOVA, interaction $p = 0.839$, challenge $p < 0.01$, treatment $p = 0.641$). There was no main effect of the challenge on blood neutrophils (Fig. 3D; two-way ANOVA, challenge $p = 0.106$), however there was a nafamostat main effect ($p < 0.05$). No post-hoc tests were significant, and there was no significant interaction ($p = 0.916$). Blood basophils (Fig. 3E; two-way ANOVA, interaction $p = 0.103$, challenge $p = 0.372$, treatment $p = 0.197$) and eosinophils (Fig. 3F; two-way ANOVA, interaction $p = 0.556$, challenge $p = 0.493$, treatment $p = 0.989$) were unaffected by both the R848 challenge and nafamostat treatment.

R848 induces systemic inflammation that is attenuated by Nafamostat

Previous work from our group has shown that the changes in the levels of mRNA for APPs correspond to changes in the levels of the APP [20, 21]; we measured mRNA levels to explore the impact of R848 and of nafamostat on the inflammatory markers. In the liver, R848 induced a significant increase in the expression of TNF (Fig. 4A; two-way ANOVA, challenge $p < 0.0001$, treatment $p = 0.075$). An interaction between the R848 challenge and nafamostat treatment approached significance ($p = 0.057$); Sidak's post-hoc test of challenged animals revealed a significant decrease in TNF expression with nafamostat treatment ($p < 0.01$). Similarly, hepatic IFN- γ expression was increased with R848 challenge (Fig. 4B; two-way ANOVA, interaction $p = 0.098$, challenge $p < 0.0001$, treatment $p = 0.114$), which was ameliorated by nafamostat (Sidak's post-hoc test, $p < 0.05$). R848 induced an increase in CXCL1 expression in the liver (Fig. 4C; two-way ANOVA, challenge $p < 0.0001$). However, there was no main effect of nafamostat ($p = 0.166$), and no interaction ($p = 0.242$). A trending decrease of CXCL1 expression in R848 animals treated with nafamostat, compared with vehicle, was observed, although this was not statistically significant (Sidak's post-hoc test, $p = 0.09$). R848 had a main effect on hepatic CXCL10 expression (Fig. 4D; two-way ANOVA, challenge $p < 0.0001$), however there was no main effect of the nafamostat ($p = 0.545$) and no interaction ($p = 0.543$). Expression of acute phase protein SAA-2 was significantly perturbed in this study (Fig. 4E; two-way ANOVA revealed a significant interaction ($p < 0.01$) and a main effect of nafamostat ($p < 0.01$), but not the challenge ($p = 0.279$). C-reactive protein (CRP), a pentraxin, was significantly increased in response to the R848 challenge (Fig. 4F; two-way ANOVA, challenge $p < 0.0001$), however there was no main effect of treatment with nafamostat ($p = 0.710$) and no interaction ($p = 0.437$). In the lung, TNF (Fig. 5A; two-way ANOVA, interaction $p = 0.666$, challenge $p < 0.0001$, treatment $p = 0.456$), IFN- γ (Fig. 5B; two-way ANOVA, interaction $p = 0.558$, challenge $p < 0.0001$, treatment $p = 0.684$), CXCL1 (Fig. 5C; two-way

ANOVA, interaction $p = 0.255$, challenge $p < 0.0001$, treatment $p = 0.106$) and CXCL10 (Fig. 5D; two-way ANOVA, interaction $p = 0.841$, challenge $p < 0.0001$, treatment $p = 0.836$) were all significantly upregulated compared both to control and to naïve animals. For lung tissue, Nafamostat had no effect on the expression of any genes analysed.

R848 induces central inflammation which is unaffected by Nafamostat treatment

The expression of pro-inflammatory genes in the prefrontal cortex of the brain was examined to understand the impact of nafamostat on R848-induced central cytokine production. Expression of TNF (Fig. 6A; two-way ANOVA, interaction $p = 0.952$, challenge $p < 0.001$, treatment $p = 0.788$), IFN- γ (Fig. 6B; two-way ANOVA, interaction $p = 0.794$, challenge $p < 0.0001$, treatment $p = 0.731$), CXCL1 (Fig. 6C; two-way ANOVA, interaction $p = 0.540$, challenge $p < 0.001$, treatment $p = 0.546$) and CXCL10 (Fig. 6D; two-way ANOVA, interaction $p > 0.999$, challenge $p < 0.0001$, treatment $p = 0.999$) were all significantly increased with the R848 challenge. Nafamostat had no effect on the expression of any of the genes examined here.

Discussion

Here, we have shown that R848 administration induces marked changes in the expression of central and peripheral cytokines, which is associated with the induction of sickness behaviour, an acute febrile response, and an acute leukocytopenia. The administration of nafamostat induced depressive-like behaviours in the FST, but there was no interaction between treatment and the behavioural measures; nafamostat administration had no significant effect on the SPT or exploration when challenged and failed to alter central cytokine production. However, nafamostat did reduce hepatic cytokine production and normalised the levels of circulating leukocytes.

It has previously been reported that R848, a TLR7/8 agonist, can induce an acute sickness behaviour phenotype [16]. Consistent with this previous study, we also observed that R848-induced an increase in body temperature, indicative of fever, and decrease in food intake. However, sickness behaviour encompasses a wider range of behavioural and physiological changes and thus we further characterised the behavioural response to the challenge. Total sucrose intake was decreased by the challenge, however there was no significant effect on sucrose preference, suggesting that R848, at this early time point does not induce anhedonia. Sucrose preference has been widely adopted to evaluate the ability of a rodent to experience pleasure [22–24] as rodents have been demonstrated to drink sweetened water avidly [25]. Although, most models of infection-associated sickness behaviour exhibit anhedonia after a 12–24 hour time period [26], and so it is plausible that an R848-induced decrease in sucrose preference may become evident at later time points. In contrast to the sucrose test, exploratory behaviour was significantly affected by R848; the number of grid crossings/minute and the total number of rears were both decreased in R848-challenged animals, which is consistent with other inflammatory models, such as those employing the classical LPS-CD14-TLR4 challenge [27]. Analysis of position in the open field revealed that the R848-treated animals chose to spend time in less in the centre of the field, which suggests that R848 had an anxiogenic effect. Increased anxiety has been reported in LPS models [27], which can be exacerbated by stress [11, 24], and is associated with central TNF expression. Collectively,

for R848, the behavioural changes observed are indicative of a sickness behaviour phenotype, and this treatment provides a useful model of ssRNA virus-induced sickness behaviour.

Currently, the PolyI:C model is widely used as a TLR3 activation model to mimic dsRNA virus infection. In particular, it has gained the most traction in modelling gestational immune activation. However, the model can generate variable results that are dependent on the source and the molecular weight of the PolyI:C used, which, coupled with age-related changes, seems to have a profound effect on the immunological outcome [28, 29]. SARS-CoV-2 can also activate TLR3 during viral replication, but mechanisms appear to have evolved to enable the virus to suppress TLR3-TRIF signalling [30]. In comparison to SARS-CoV and MERS-CoV, whole-genome sequencing of SARS-CoV-2 has revealed that TLR7 is likely to be of particular importance in pathogenesis of SARS-CoV-2 as it has more ssRNA motifs that could bind to TLR7 [31]. Furthermore, loss-of-function variants of X-chromosomal TLR7 have been identified in young male patients with severe COVID-19 [32]. Thus, the use of R848 presents a useful opportunity to understand the impact of TLR7 activation on behaviour and the systemic inflammatory response in viral illnesses.

Analysis of the FST data did not reveal any R848-mediated effect, as both latency to float and total float time were both unaffected by the challenge. This is, perhaps, not surprising as the FST is a measure of helplessness [33], which is not often associated with sickness behaviour. Indeed, previous studies with an LPS challenge were similarly unable to demonstrate consistent changes in this test [34]. The FST is widely used to measure the efficacy of potential anti-depressant therapy [33], however interpretation of the results is controversial. Whilst increased immobility is thought to reflect a depressive-state, this response could similarly suggest habituation and learning [35], which are often perceived as a adaptive behavioural response. While the FST may not be a good indicator of sickness behaviour, there was a significant main effect of nafamostat on the total float time, suggesting that nafamostat does have some unexpected behavioural effects.

Leukocytosis is commonly observed in response to infection. Therefore, it was surprising to note that the R848 challenge induced depletion of circulating leukocytes, and, more specifically, in circulating lymphocytes. Although unexpected, this is not a unique observation; a decrease in blood lymphocytes has been reported in patients and in animal models of acute viral infection [36–38], including after TLR7 stimulation [39]. Interestingly, clinical studies have reported a decrease in CD4 + and CD8 + T lymphocyte counts in COVID-19 patients [40, 41], and, therefore, the effects of R848 could be recapitulating the lymphopenia observed in this disease. The mechanism by which this depletion occurs is unclear, although it may be owing to widespread sequestration in peripheral organs. It is known that leukocytes infiltrate peripheral organs to locate the source of infection [27, 38], as such our result may reflect this infiltration, which is occurring more rapidly than cell replacement from lymphoid organs. Alternatively, lymphocytes may be undergoing increased cell death. Diao et al. [41] showed that remaining T-cells from COVID-19 patients had increased levels of PD-1, a protein surface marker that promotes apoptosis. Critically, leukocyte depletion was normalised by treatment with nafamostat. Given that the magnitude of

lymphocyte depletion was associated with disease severity [41], this result suggests that nafamostat treatment may reduce the severity of COVID-19 and improve patient outcomes.

The magnitude of systemic inflammatory response was evaluated by measuring the relative expression of pro-inflammatory genes in the liver and lung [42]. In both organs, the R848 challenge induced a significant increase in TNF, IFN- γ , CXCL1 and CXCL10. In addition, the acute phase proteins SAA-2 and CRP expression were elevated. These inflammatory mediators have long been associated with viral infection and the induction of sickness behaviour [43]. TLR7 is strongly expressed by macrophages [44], and it seems probable that it is the resident tissue macrophages that are responsible for producing these cytokines [45], which would also account for the differential expression levels between the organs, as there is a greater density of macrophages in the liver than the lung. Here, we were also able to show that nafamostat had a peripheral anti-inflammatory effect; hepatic TNF and IFN- γ expression, induced by R848, was significantly ameliorated by nafamostat treatment, as well as CXCL1 to a lesser extent. As this model does not employ live virus, and, instead, triggers an immune response via TLR7/8 activation, this highlights the utility of nafamostat as a broad-spectrum serine protease inhibitor that is able to suppress the inflammatory response, independent of viral cell entry. Certainly, serine proteases have been implicated as moderators of inflammation by regulating cytokine and chemokine expression [46]. For example, neutrophil-derived Cathepsin G is a serine protease, which stimulates IFN- γ production and cleaves membrane-bound TNF- α [47], although it is acknowledged that the IC₅₀ is much higher for Cathepsin G than for TMPRSS2. Many enzymes of the complement cascade, including C1r and C1s, are also in the serine protease family [48]. Therefore, nafamostat may be acting upon any number of alternative endogenous enzymes to cause the observed anti-inflammatory effect.

Despite the attenuation of the hepatic inflammatory response, nafamostat treatment had no effect on brain cytokine expression. We, and others, have shown that a peripheral inflammatory challenge induces a central cytokine response in the CNS [26]. In keeping with this, systemic administration of R848 induced pro-inflammatory gene expression in the prefrontal cortex of the brain, including a 400-fold increase in CXCL10 expression. Although, it remains unknown precisely how signals from the periphery result in central cytokine production [17] or whether, in this case, R848 is able to activate central TLR7 directly. As it has been shown that nafamostat is unable to cross the BBB [49], it seems likely that it is the absence of any CNS bioavailability that resulted in no change in central cytokine expression observed in this study. Nafamostat is also metabolised and cleared *in vivo* with a half-life of 23 minutes [50], which would further prevent appreciable accumulation of nafamostat in the brain. Despite this, we have previously shown that inhibition of TNF signalling in the periphery can attenuate sickness behaviours induced by the central injection of interleukin-1b [51, 52], and we might have expected some attenuation of the response. Although, timing may be an issue. Duan et al. [6] showed that nafamostat reduced expression of pro-inflammatory cytokines in the spinal cord after traumatic injury, however authors evaluated levels 24 hours post-injury, whilst in this study, brains were collected 6 hours post-challenge. Additional later time points, or a multi-dose treatment regime could be explored to investigate this.

Clinical trials investigating the efficacy of nafamostat in the treatment of COVID-19 are currently underway. Whilst its primary mechanism of action is proposed to be inhibition of TMPRSS2 and subsequent viral entry, data in this study suggests that nafamostat has may have additional beneficial anti-inflammatory effects, which may be beneficial in the treatment of COVID-19. Nafamostat may also limit disease associated coagulopathy and improve patient survival. As highlighted previously, nafamostat is currently approved to treat pancreatitis, and so it has a proven safety record. This, combined with its known pharmacokinetics, indicates that repurposing it for the treatment of COVID-19 could be rapid and straightforward.

Conclusion

A single injection of the TLR7/8 agonist R848 generates systemic and central inflammation and sickness behaviours, which is amenable to therapeutic intervention. Given that R848 is a small molecule agonist, and not a live virus, this model provides a safe and simple tool to investigate therapy designed to ameliorate inappropriate and excessive TLR7 activation, and to understand the impact of TLR7 activation on affect. The serine protease inhibitor nafamostat was able to attenuate peripheral inflammation and normalise circulating leukocyte numbers in this model. As these results were achieved in the absence of viral entry, we propose that nafamostat may have useful anti-inflammatory effects, which may be advantageous in the treatment of viral infections, including COVID-19.

List Of Abbreviations

ACE2 Angiotensin-converting enzyme 2

ANOVA Analysis of variance

COVID-19 Coronavirus disease 2019

APR Acute phase response

MERS Middle East respiratory syndrome

PRR Pattern recognition receptor

TLR Toll-like receptor

SARS Severe acute respiratory syndrome

SARS-CoV2 Severe acute respiratory syndrome coronavirus 2

SEM Standard error of the mean

TMPRSS2 Type 2 transmembrane serine protease

Declarations

Ethics approval and consent to participate

All experiments were approved by the University of Oxford local committees (LERP, ACER) in accordance with the UK Animals (Scientific Procedures) Act 1989.

Consent for publication

Not Applicable.

Availability of data and material

All data generated during and/or analysed during the current study are included in this published article.

Competing interests

The authors declare that they have no competing interests.

Funding

AY is supported by the Nathalie Rose Barr Award from International Spinal Research Trust. DA is supported by the UK MRC under grant MC-PC-15029.

Author's contributions

AY, TS and DA designed the study. AY performed all licensed procedures. Behaviour and qPCR analysis were completed by AY, CW and YY; white blood cell analysis was completed by YY. The manuscript was written by AY, CW and YY, and edited by AY, TS and DA. All authors read and approved the final manuscript.

Acknowledgements

We would like to thank Dr Yvonne Couch for her input for the manuscript.

References

1. Hoffmann M, Kleine-Weber H, Schroeder S, Kruger N, Herrler T, Erichsen S, Schiergens TS, Herrler G, Wu NH, Nitsche A, et al: **SARS-CoV-2 Cell Entry Depends on ACE2 and TMPRSS2 and Is Blocked by a Clinically Proven Protease Inhibitor.** *Cell* 2020, **181**:271-280 e278.
2. Yamamoto M, Kiso M, Sakai-Tagawa Y, Iwatsuki-Horimoto K, Imai M, Takeda M, Kinoshita N, Ohmagari N, Gohda J, Semba K, et al: **The Anticoagulant Nafamostat Potently Inhibits SARS-CoV-2 S Protein-Mediated Fusion in a Cell Fusion Assay System and Viral Infection In Vitro in a Cell-Type-Dependent Manner.** *Viruses* 2020, **12**.

3. Yamamoto M, Matsuyama S, Li X, Takeda M, Kawaguchi Y, Inoue JI, Matsuda Z: **Identification of Nafamostat as a Potent Inhibitor of Middle East Respiratory Syndrome Coronavirus S Protein-Mediated Membrane Fusion Using the Split-Protein-Based Cell-Cell Fusion Assay.** *Antimicrob Agents Chemother* 2016, **60**:6532-6539.
4. Takahashi W, Yoneda T, Koba H, Ueda T, Tsuji N, Ogawa H, Asakura H: **Potential mechanisms of nafamostat therapy for severe COVID-19 pneumonia with disseminated intravascular coagulation.** *Int J Infect Dis* 2021, **102**:529-531.
5. Liu Y, Li C, Wang J, Fang Y, Sun H, Tao X, Zhou XF, Liao H: **Nafamostat Mesilate Improves Neurological Outcome and Axonal Regeneration after Stroke in Rats.** *Mol Neurobiol* 2017, **54**:4217-4231.
6. Duan HQ, Wu QL, Yao X, Fan BY, Shi HY, Zhao CX, Zhang Y, Li B, Sun C, Kong XH, et al: **Nafamostat mesilate attenuates inflammation and apoptosis and promotes locomotor recovery after spinal cord injury.** *CNS Neurosci Ther* 2018, **24**:429-438.
7. Marotta F, Fesce E, Rezakovic I, Chui DH, Suzuki K, Ideo G: **Nafamostat mesilate on the course of acute pancreatitis. Protective effect on peritoneal permeability and relation with supervening pulmonary distress.** *Int J Pancreatol* 1994, **16**:51-59.
8. Lu YC, Yeh WC, Ohashi PS: **LPS/TLR4 signal transduction pathway.** *Cytokine* 2008, **42**:145-151.
9. Campbell SJ, Anthony DC, Oakley F, Carlsen H, Elsharkawy AM, Blomhoff R, Mann DA: **Hepatic nuclear factor kappa B regulates neutrophil recruitment to the injured brain.** *J Neuropathol Exp Neurol* 2008, **67**:223-230.
10. Kelley KW, Bluthé RM, Dantzer R, Zhou JH, Shen WH, Johnson RW, Broussard SR: **Cytokine-induced sickness behavior.** *Brain Behav Immun* 2003, **17 Suppl 1**:S112-118.
11. Couch Y, Anthony DC, Dolgov O, Revischin A, Festoff B, Santos AI, Steinbusch HW, Strekalova T: **Microglial activation, increased TNF and SERT expression in the prefrontal cortex define stress-altered behaviour in mice susceptible to anhedonia.** *Brain Behav Immun* 2013, **29**:136-146.
12. Cunningham C, Champion S, Teeling J, Felton L, Perry VH: **The sickness behaviour and CNS inflammatory mediator profile induced by systemic challenge of mice with synthetic double-stranded RNA (poly I:C).** *Brain Behav Immun* 2007, **21**:490-502.
13. Monguio-Tortajada M, Franquesa M, Sarrias MR, Borrás FE: **Low doses of LPS exacerbate the inflammatory response and trigger death on TLR3-primed human monocytes.** *Cell Death Dis* 2018, **9**:499.
14. Machhi J, Herskovitz J, Senan AM, Dutta D, Nath B, Oleynikov MD, Blomberg WR, Meigs DD, Hasan M, Patel M, et al: **The Natural History, Pathobiology, and Clinical Manifestations of SARS-CoV-2 Infections.** *J Neuroimmune Pharmacol* 2020, **15**:359-386.

15. Jefferies CA: **Regulating IRFs in IFN Driven Disease.** *Front Immunol* 2019, **10**:325.
16. Michaelis KA, Norgard MA, Levasseur PR, Olson B, Burfeind KG, Buenafe AC, Zhu X, Jeng S, McWeeney SK, Marks DL: **Persistent Toll-like receptor 7 stimulation induces behavioral and molecular innate immune tolerance.** *Brain Behav Immun* 2019, **82**:338-353.
17. Dantzer R: **Cytokine, sickness behavior, and depression.** *Immunol Allergy Clin North Am* 2009, **29**:247-264.
18. Hart BL: **Biological basis of the behavior of sick animals.** *Neurosci Biobehav Rev* 1988, **12**:123-137.
19. Couch Y, Akbar N, Roodselaar J, Evans MC, Gardiner C, Sargent I, Romero IA, Bristow A, Buchan AM, Haughey N, Anthony DC: **Circulating endothelial cell-derived extracellular vesicles mediate the acute phase response and sickness behaviour associated with CNS inflammation.** *Sci Rep* 2017, **7**:9574.
20. Campbell SJ, Hughes PM, Iredale JP, Wilcockson DC, Waters S, Docagne F, Perry VH, Anthony DC: **CINC-1 is an acute-phase protein induced by focal brain injury causing leukocyte mobilization and liver injury.** *FASEB J* 2003, **17**:1168-1170.
21. Campbell SJ, Perry VH, Pitossi FJ, Butchart AG, Chertoff M, Waters S, Dempster R, Anthony DC: **Central nervous system injury triggers hepatic CC and CXC chemokine expression that is associated with leukocyte mobilization and recruitment to both the central nervous system and the liver.** *Am J Pathol* 2005, **166**:1487-1497.
22. Antoniuk S, Bijata M, Ponimaskin E, Wlodarczyk J: **Chronic unpredictable mild stress for modeling depression in rodents: Meta-analysis of model reliability.** *Neurosci Biobehav Rev* 2019, **99**:101-116.
23. Levine R: **Genetic relationships, choice models, and sucrose preference behaviour in mice.** *Nature* 1967, **215**:668-669.
24. Couch Y, Trofimov A, Markova N, Nikolenko V, Steinbusch HW, Chekhonin V, Schroeter C, Lesch KP, Anthony DC, Strekalova T: **Low-dose lipopolysaccharide (LPS) inhibits aggressive and augments depressive behaviours in a chronic mild stress model in mice.** *J Neuroinflammation* 2016, **13**:108.
25. Strekalova T, Steinbusch HW: **Measuring behavior in mice with chronic stress depression paradigm.** *Prog Neuropsychopharmacol Biol Psychiatry* 2010, **34**:348-361.
26. Couch Y, Xie Q, Lundberg L, Sharp T, Anthony DC: **A Model of Post-Infection Fatigue Is Associated with Increased TNF and 5-HT_{2A} Receptor Expression in Mice.** *PLoS One* 2015, **10**:e0130643.
27. Couch Y, Davis AE, Sa-Pereira I, Campbell SJ, Anthony DC: **Viral pre-challenge increases central nervous system inflammation after intracranial interleukin-1 β injection.** *J Neuroinflammation* 2014,

11:178.

28. McGarry N, Murray CL, Garvey S, Wilkinson A, Tortorelli L, Ryan L, Hayden L, Healy D, Griffin EW, Hennessy E, et al: **Double stranded RNA drives innate immune responses, sickness behavior and cognitive impairment dependent on dsRNA length, IFNAR1 expression and age.** *bioRxiv* 2021.
29. Careaga M, Taylor SL, Chang C, Chiang A, Ku KM, Berman RF, Van de Water JA, Bauman MD: **Variability in PolyIC induced immune response: Implications for preclinical maternal immune activation models.** *J Neuroimmunol* 2018, **323**:87-93.
30. Han L, Zhuang MW, Deng J, Zheng Y, Zhang J, Nan ML, Zhang XJ, Gao C, Wang PH: **SARS-CoV-2 ORF9b antagonizes type I and III interferons by targeting multiple components of the RIG-I/MDA-5-MAVS, TLR3-TRIF, and cGAS-STING signaling pathways.** *J Med Virol* 2021.
31. Moreno-Eutimio MA, Lopez-Macias C, Pastelin-Palacios R: **Bioinformatic analysis and identification of single-stranded RNA sequences recognized by TLR7/8 in the SARS-CoV-2, SARS-CoV, and MERS-CoV genomes.** *Microbes Infect* 2020, **22**:226-229.
32. van der Made CI, Simons A, Schuurs-Hoeijmakers J, van den Heuvel G, Mantere T, Kersten S, van Deuren RC, Steehouwer M, van Reijmersdal SV, Jaeger M, et al: **Presence of Genetic Variants Among Young Men With Severe COVID-19.** *JAMA* 2020, **324**:663-673.
33. Kraeuter AK, Guest PC, Sarnyai Z: **The Forced Swim Test for Depression-Like Behavior in Rodents.** *Methods Mol Biol* 2019, **1916**:75-80.
34. Deak T, Bellamy C, D'Agostino LG, Rosanoff M, McElderry NK, Bordner KA: **Behavioral responses during the forced swim test are not affected by anti-inflammatory agents or acute illness induced by lipopolysaccharide.** *Behav Brain Res* 2005, **160**:125-134.
35. Commons KG, Cholanians AB, Babb JA, Ehlinger DG: **The Rodent Forced Swim Test Measures Stress-Coping Strategy, Not Depression-like Behavior.** *ACS Chem Neurosci* 2017, **8**:955-960.
36. Perez-Padilla R, de la Rosa-Zamboni D, Ponce de Leon S, Hernandez M, Quinones-Falconi F, Bautista E, Ramirez-Venegas A, Rojas-Serrano J, Ormsby CE, Corrales A, et al: **Pneumonia and respiratory failure from swine-origin influenza A (H1N1) in Mexico.** *N Engl J Med* 2009, **361**:680-689.
37. Boonnak K, Vogel L, Feldmann F, Feldmann H, Legge KL, Subbarao K: **Lymphopenia associated with highly virulent H5N1 virus infection due to plasmacytoid dendritic cell-mediated apoptosis of T cells.** *J Immunol* 2014, **192**:5906-5912.
38. Li T, Qiu Z, Zhang L, Han Y, He W, Liu Z, Ma X, Fan H, Lu W, Xie J, et al: **Significant changes of peripheral T lymphocyte subsets in patients with severe acute respiratory syndrome.** *J Infect Dis* 2004, **189**:648-651.

39. Gunzer M, Riemann H, Basoglu Y, Hillmer A, Weishaupt C, Balkow S, Benninghoff B, Ernst B, Steinert M, Scholzen T, et al: **Systemic administration of a TLR7 ligand leads to transient immune incompetence due to peripheral-blood leukocyte depletion.** *Blood* 2005, **106**:2424-2432.
40. Chen G, Wu D, Guo W, Cao Y, Huang D, Wang H, Wang T, Zhang X, Chen H, Yu H, et al: **Clinical and immunological features of severe and moderate coronavirus disease 2019.** *J Clin Invest* 2020, **130**:2620-2629.
41. Diao B, Wang C, Tan Y, Chen X, Liu Y, Ning L, Chen L, Li M, Liu Y, Wang G, et al: **Reduction and Functional Exhaustion of T Cells in Patients With Coronavirus Disease 2019 (COVID-19).** *Front Immunol* 2020, **11**:827.
42. Campbell SJ, Meier U, Mardiguian S, Jiang Y, Littleton ET, Bristow A, Relton J, Connor TJ, Anthony DC: **Sickness behaviour is induced by a peripheral CXC-chemokine also expressed in multiple sclerosis and EAE.** *Brain Behav Immun* 2010, **24**:738-746.
43. Biesmans S, Meert TF, Bouwknecht JA, Acton PD, Davoodi N, De Haes P, Kuijlaars J, Langlois X, Matthews LJ, Ver Donck L, et al: **Systemic immune activation leads to neuroinflammation and sickness behavior in mice.** *Mediators Inflamm* 2013, **2013**:271359.
44. Alothaimen T, Trus E, Basta S, Gee K: **Differential TLR7-mediated cytokine expression by R848 in M-CSF- versus GM-CSF-derived macrophages after LCMV infection.** *J Gen Virol* 2021, **102**.
45. Campbell SJ, Zahid I, Losey P, Law S, Jiang Y, Bilgen M, van Rooijen N, Morsali D, Davis AE, Anthony DC: **Liver Kupffer cells control the magnitude of the inflammatory response in the injured brain and spinal cord.** *Neuropharmacology* 2008, **55**:780-787.
46. Safavi F, Rostami A: **Role of serine proteases in inflammation: Bowman-Birk protease inhibitor (BBI) as a potential therapy for autoimmune diseases.** *Exp Mol Pathol* 2012, **93**:428-433.
47. Burster T, Macmillan H, Hou T, Boehm BO, Mellins ED: **Cathepsin G: roles in antigen presentation and beyond.** *Mol Immunol* 2010, **47**:658-665.
48. Sim RB, Laich A: **Serine proteases of the complement system.** *Biochem Soc Trans* 2000, **28**:545-550.
49. Chen X, Li M, Xiong ZG, Orser BA, Macdonald JF, Lu WY: **An anti-coagulation agent Futhan preferentially targets GABA(A) receptors in lung epithelia: implication in treating asthma.** *Int J Physiol Pathophysiol Pharmacol* 2011, **3**:249-256.
50. Tsukagoshi S: **[Pharmacokinetics studies of nafamostat mesilate (FUT), a synthetic protease inhibitor, which has been used for the treatments of DIC and acute pancreatitis, and as an anticoagulant in extracorporeal circulation].** *Gan To Kagaku Ryoho* 2000, **27**:767-774.

51. Campbell SJ, Jiang Y, Davis AE, Farrands R, Holbrook J, Leppert D, Anthony DC: **Immunomodulatory effects of etanercept in a model of brain injury act through attenuation of the acute-phase response.** *J Neurochem* 2007, **103**:2245-2255.
52. Jiang Y, Deacon R, Anthony DC, Campbell SJ: **Inhibition of peripheral TNF can block the malaise associated with CNS inflammatory diseases.** *Neurobiol Dis* 2008, **32**:125-132.

Figures

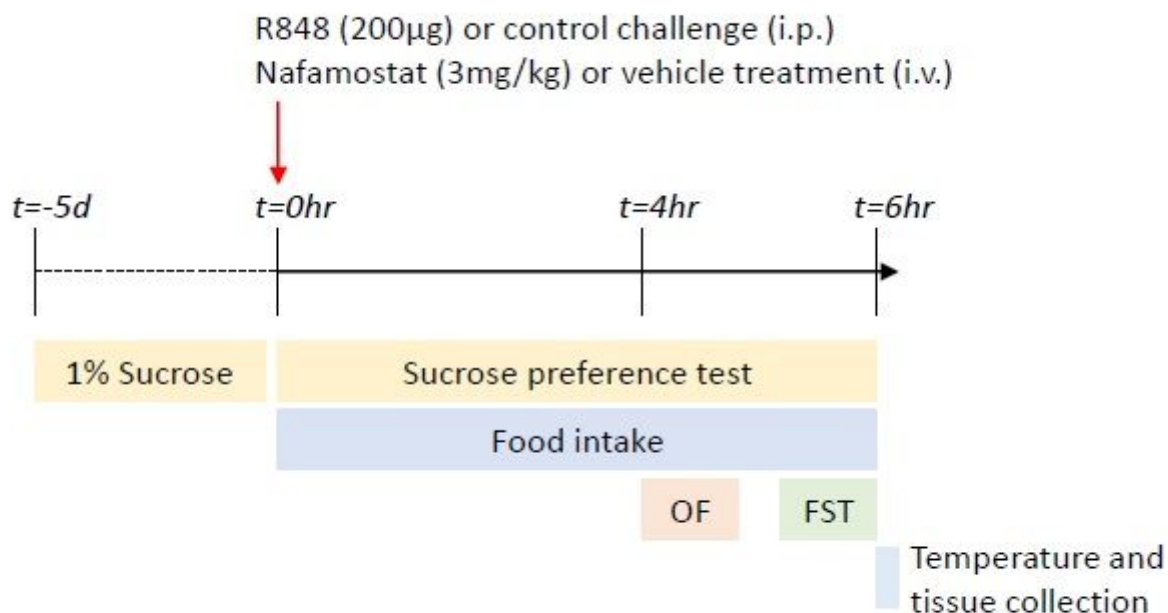


Figure 1

Schematic of behavioural tests performed. In summary, animals were exposed to 1% sucrose solution during the 5 days of acclimatisation. On the day of the experiment, male, CD-1 mice received an intraperitoneal injection of R848 (200 µg, dissolved in DMSO and sterile saline) or control solution (DMSO diluted in sterile saline), together with an intravenous injection of nafamostat (3 mg/kg) or vehicle (sterile saline). For the duration of the experiment, animals underwent the sucrose preference test (SPT), and food intake was examined. 4 hours post-challenge, animals completed the open field (OF) paradigm. 6 hours post-challenge, animals completed the forced swim test (FST), after which their temperature was determined and animals were culled. d=days, hr=hours.

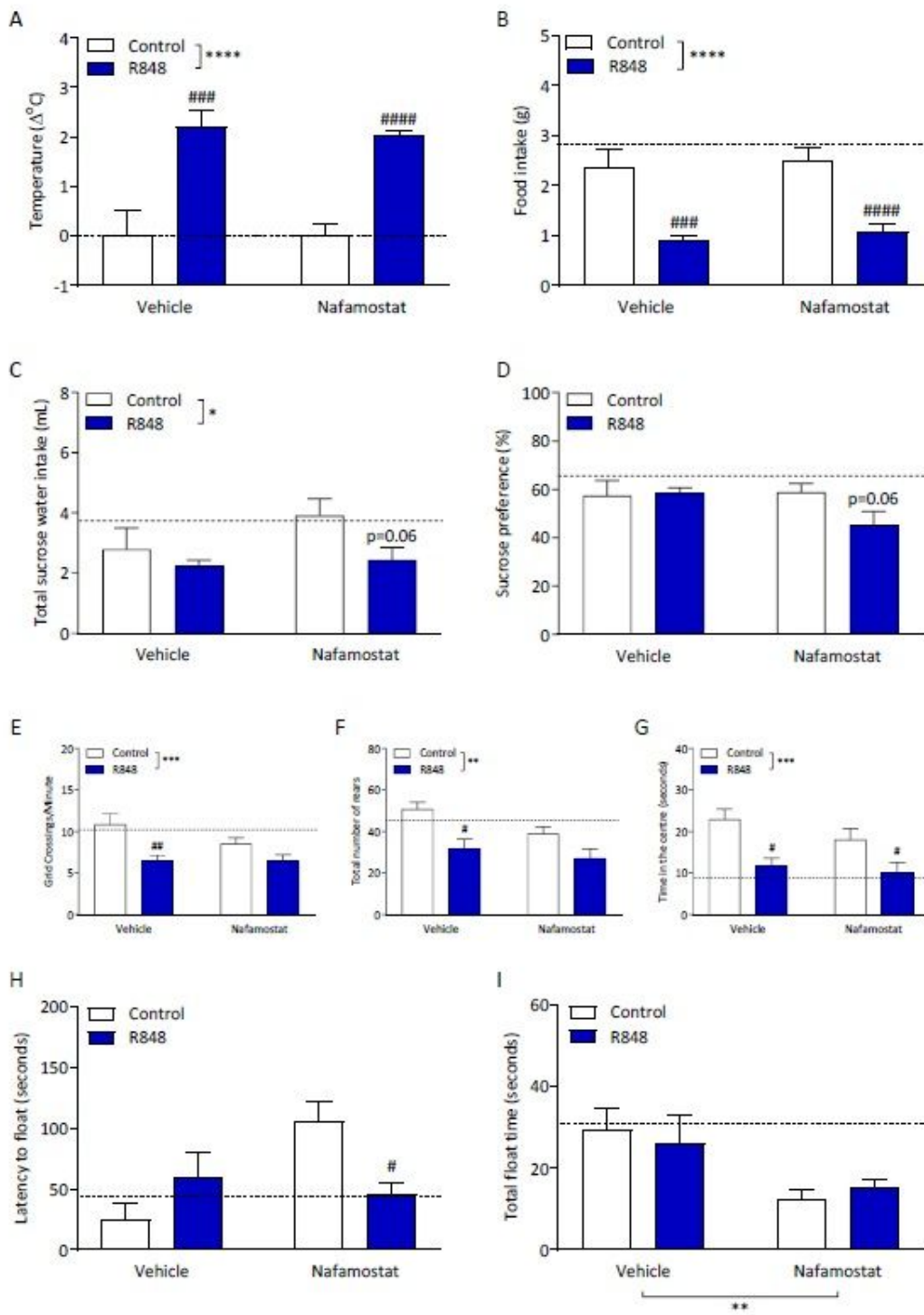


Figure 2

R848 induces a sickness behaviour phenotype, which is not ameliorated by nafamostat. Male, CD-1 mice received an intraperitoneal injection of R848 (200 μg , dissolved in DMSO and sterile saline) or control solution (DMSO diluted in sterile saline), together with an intravenous injection of nafamostat (3mg/kg) or vehicle (sterile saline), and sickness behaviour was assessed 4-6 hours later. Animal temperature (A) and food intake (B) were determined to assess any fever and anorexia, respectively. Anhedonia was

measured with the SPT; total sucrose water intake (C) and preference for the sucrose water (D) were evaluated. OF was used to assess exploratory behaviour and grid crossings/minute (F), number of rears (G) and time spent in the centre (H) were calculated. Latency to immobility (H) and total immobility (I) in the FST were measured. Naïve animals were included to establish baseline (dotted line). Data presented as mean \pm SEM, $n=4-10$ /group, and analysed by two-way ANOVA, $*p<0.05$, $**p<0.01$, $***p<0.001$, $****p<0.0001$ main effect, $\#p<0.05$, $\#\#p<0.01$, $\#\#\#p<0.001$, $\#\#\#\#p<0.0001$ control vs. R848 in Sidak's post-hoc test.

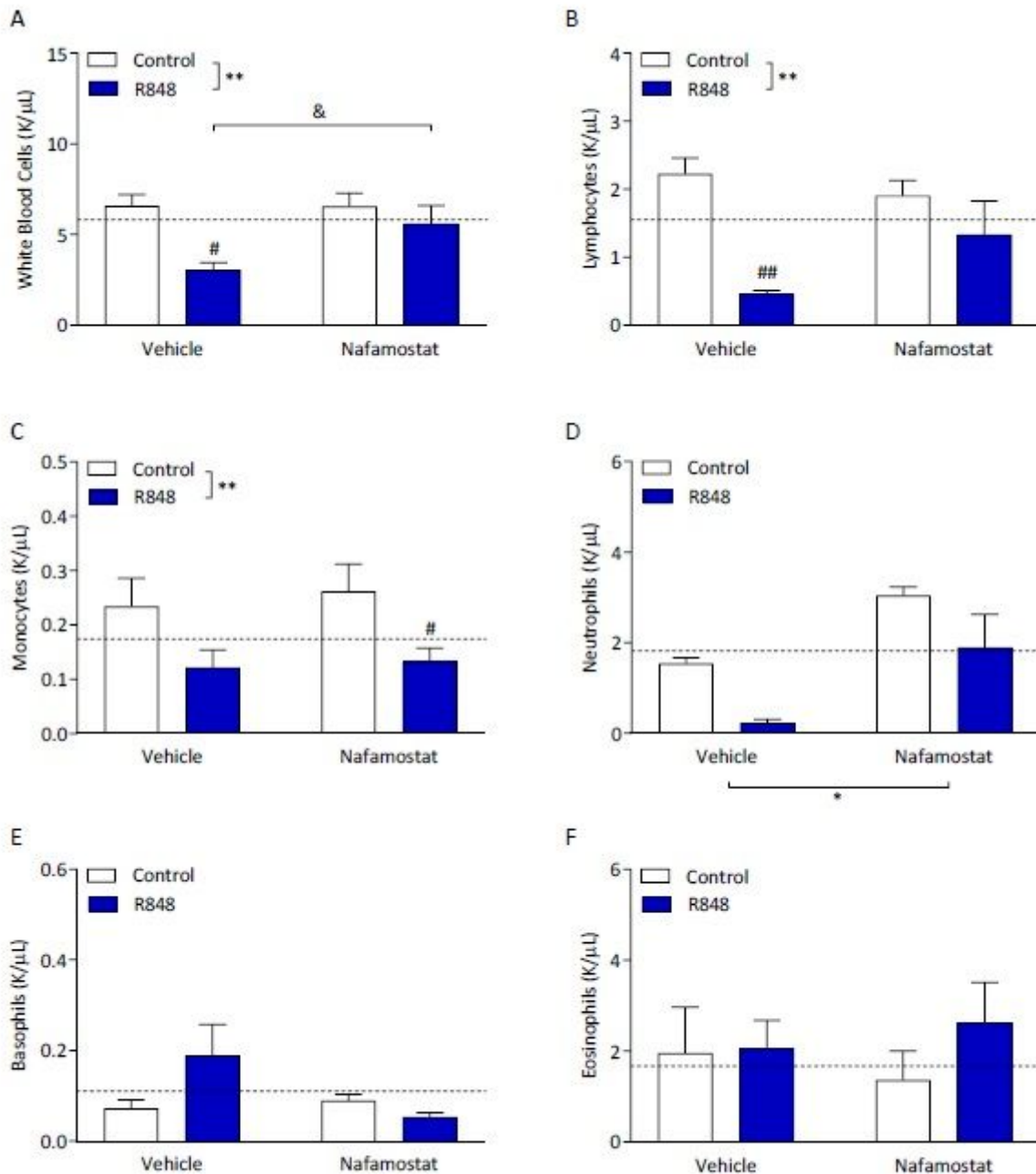


Figure 3

R848 causes a depletion in circulating leukocytes, which is partially restored by nafamostat. Male, CD-1 mice received an intraperitoneal injection of R848 (200µg, dissolved in DMSO and sterile saline) or control solution (DMSO diluted in sterile saline), together with an intravenous injection of nafamostat (3mg/kg) or vehicle (sterile saline). Blood was collected 6 hours post-challenge and total concentration of total white blood cells (A), as well as the concentrations of lymphocytes (B), monocytes (C), neutrophils (D), basophils (E) and eosinophils (F), specifically, were measured. Naïve animals were included to establish baseline (dotted line). Data presented as mean ±SEM, n=4-10/group, and analysed by two-way ANOVA, **p<0.01 main effect, #p<0.05, ##p<0.01 control vs. R848 with Sidak's post-hoc test, &p<0.05 vehicle vs. nafamostat with Sidak's post-hoc test.

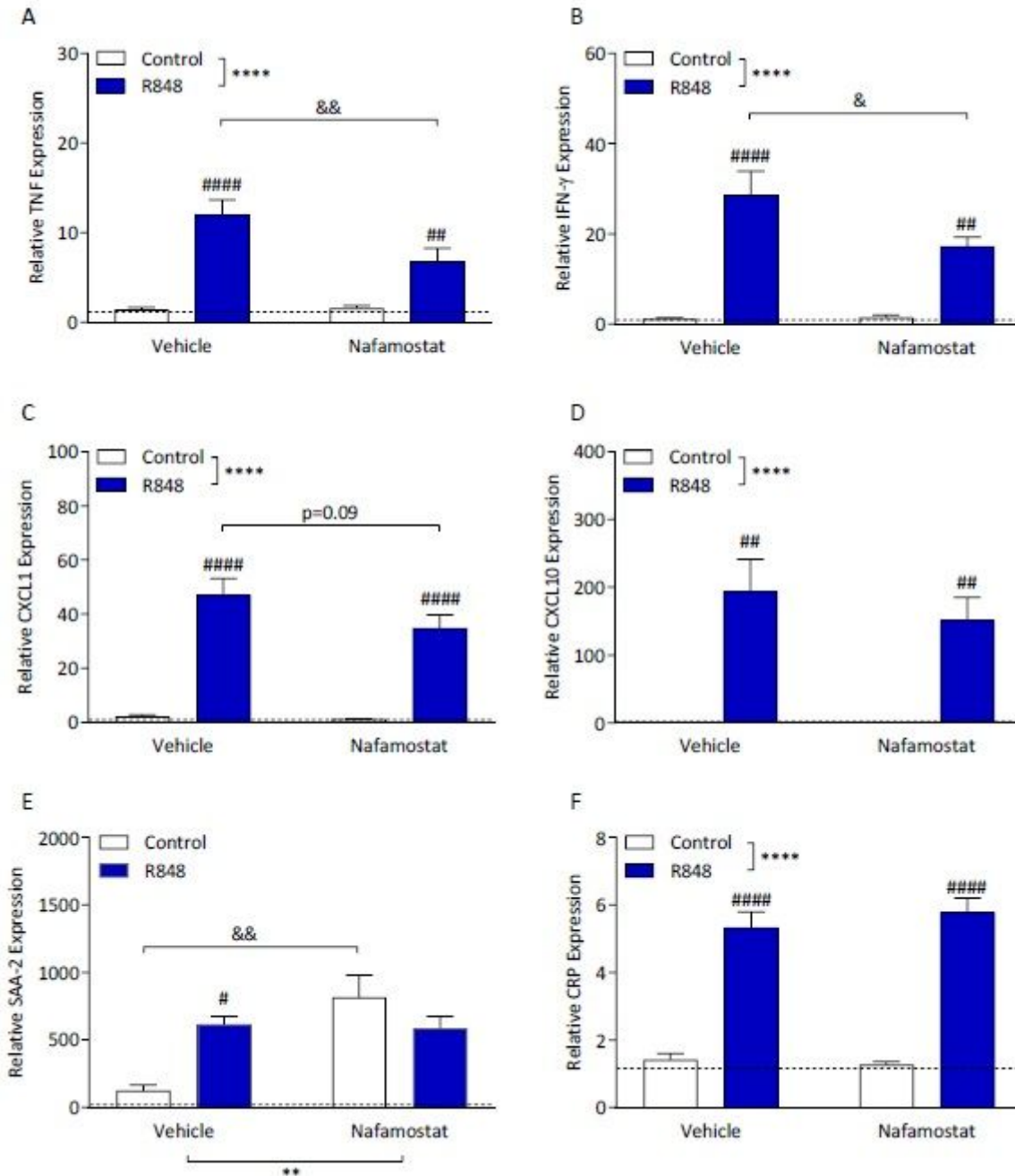


Figure 4

R848 induces pro-inflammatory gene expression in the liver, which is ameliorated with nafamostat treatment. Male, CD-1 mice received an intraperitoneal injection of R848 (200µg, dissolved in DMSO and sterile saline) or control solution (DMSO diluted in sterile saline), together with an intravenous injection of nafamostat (3mg/kg) or vehicle (sterile saline). Fresh liver was collected 6 hours post-challenge and relative expression of TNF (A), IFN-γ (B), CXCL1 (C), CXCL10 (D), SAA-2 (E) and CRP (F) were determined by qPCR. Naïve animals were included to establish baseline (dotted line). Data presented as mean ± SEM, n=4-10/group, and analysed by two-way ANOVA, ****p<0.0001 main effect, ##p<0.01, ####p<0.0001 control vs. R848 with Sidak's post-hoc test, &p<0.05, &&p<0.01 vehicle vs. nafamostat with Sidak's post-hoc test.

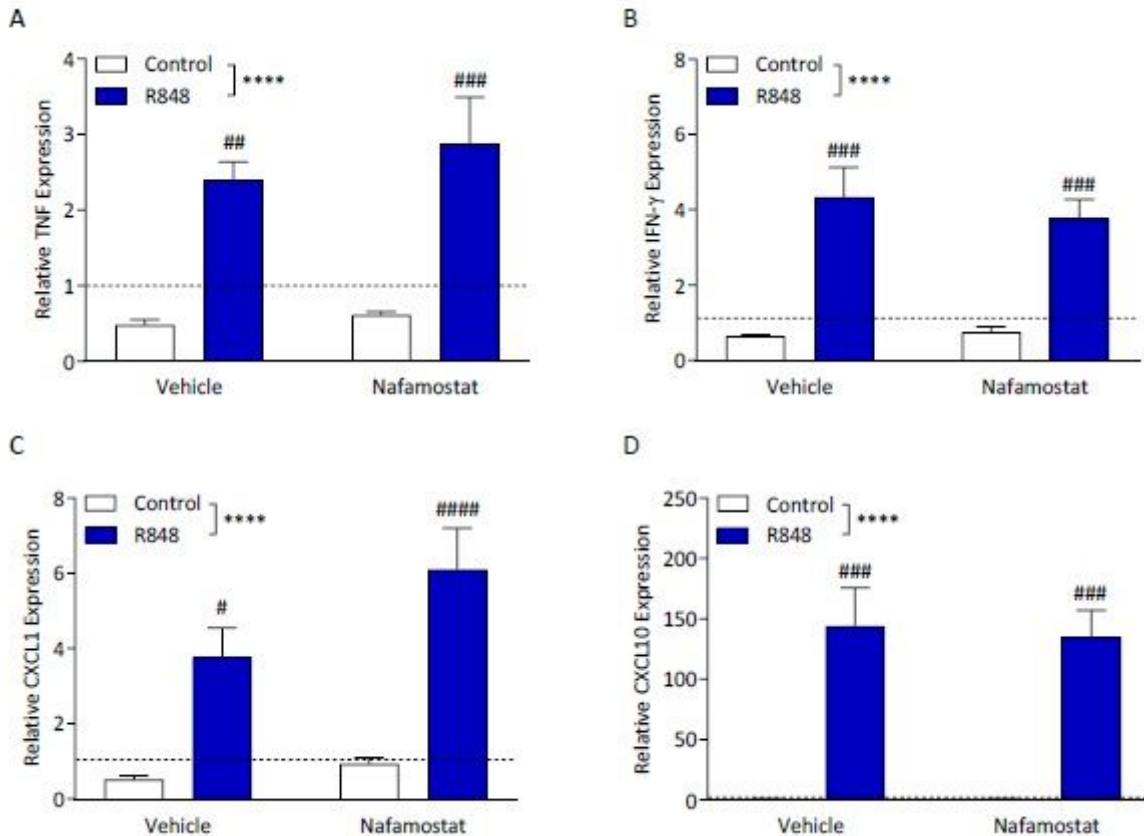


Figure 5

R848 induces pro-inflammatory gene expression in the lung, which is unaffected by treatment with nafamostat. Male, CD-1 mice received an intraperitoneal injection of R848 (200µg, dissolved in DMSO and sterile saline) or control solution (DMSO diluted in sterile saline), together with an intravenous injection of nafamostat (3mg/kg) or vehicle (sterile saline). Fresh lung was collected 6 hours post-challenge and relative expression of TNF (A), IFN-γ (B), CXCL1 (C) and CXCL10 (D) were determined by qPCR. Naïve animals were included to establish baseline (dotted line). Data presented as mean ± SEM, n=4-10/group, and analysed by two-way ANOVA, ****p<0.0001 main effect, #p<0.05, ##p<0.01, ###p<0.001 control vs. R848 with Sidak's post-hoc test.

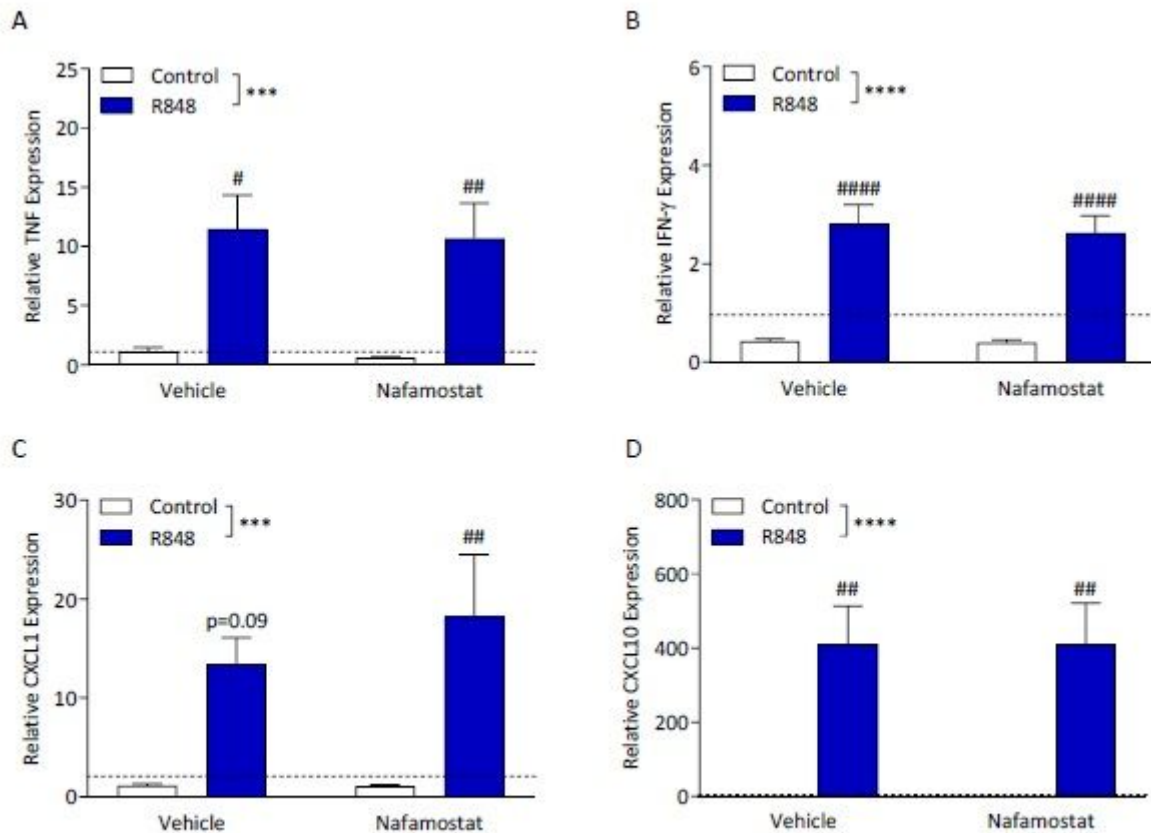


Figure 6

R848 causes pro-inflammatory gene expression in the brain which is not attenuated by nafamostat. Male, CD-1 mice received an intraperitoneal injection of R848 (200µg, dissolved in DMSO and sterile saline) or control solution (DMSO diluted in sterile saline), together with an intravenous injection of nafamostat (3mg/kg) or vehicle (sterile saline). Fresh brain was collected 6 hours post-challenge. Relative expression of TNF (A), IFN-γ (B), CXCL1 (C) and CXCL10 (D) in the prefrontal cortex were determined by qPCR. Naïve animals were included to establish baseline (dotted line). Data presented as mean ±SEM, n=4-10/group, and analysed by two-way ANOVA, ***p<0.001, ****p<0.0001 main effect, #p<0.05, ##p<0.01, ###p<0.001 control vs. R848 with Sidak's post-hoc test.